

Original Article

Brain findings associated with risperidone in rhesus monkeys: magnetic resonance imaging and pathology perspectives

Guillermo Fernandez^{1*}, Sabu Kuruvilla^{1*}, Catherine D. G. Hines², Frédéric Poignant³, James Marr⁴, Thomas Forest¹, and Richard Briscoe¹

¹ Safety Assessment and Laboratory Animal Resources, Merck & Co., Inc., 770 Sumneytown Pike, West Point, PA 19486, USA

² Translational Imaging Biomarkers, Merck & Co., Inc., 770 Sumneytown Pike, West Point, PA 19486, USA

³ Safety Assessment and Laboratory Animal Resources, Laboratoires Merck Sharp & Dohme-Chibret, Route de Marsat - Riom, 63963 Clermont-Ferrand cedex 9, France

⁴ Pharmacokinetics, Pharmacodynamics and Drug Metabolism, Merck & Co., Inc., 770 Sumneytown Pike, West Point, PA 19486, USA

Abstract: Brain changes associated with risperidone, a dopamine-2/serotonin-2 receptor antagonist, have been documented in rats and humans, but not in nonhuman primates. This study characterized brain changes associated with risperidone in nonhuman primates. Rhesus monkeys were orally administered risperidone in a dose-escalation paradigm up to a maximum tolerated dose of 0.5 mg/kg/day for 3 weeks, or 3 months followed by a 3-month recovery period. Transient and fully reversible neurological signs consistent with risperidone pharmacology were observed. The results of a magnetic resonance imaging evaluation after 3 months of treatment and at the end of the 3-month recovery period showed no meaningful changes in the brain. There were no risperidone-related brain weight changes or gross findings. Histomorphological evaluation of brain sections stained with hematoxylin and eosin, ionized calcium binding adaptor molecule 1 (Iba1), and luxol fast blue/cresyl violet double staining showed no notable differences between control and risperidone groups. However, evaluation of the brain after glial fibrillary acidic protein (GFAP) immunohistochemical staining revealed increased staining in the cell bodies and processes of astrocytes in the putamen without apparent alterations in numbers or distribution. The increase in GFAP staining was present after 3 weeks and 3 months of treatment, but no increase in staining was observed after the 3-month recovery period, demonstrating the reversibility of this finding. The reversible increase in GFAP expression was likely an adaptive, non-adverse response of astrocytes, associated with the pharmacology of risperidone. These observations are valuable considerations in the nonclinical risk assessment of new drug candidates for psychiatric disorders. (DOI: 10.1293/tox.2019-0004; *J Toxicol Pathol* 2019; 32: 233–243)

Key words: risperidone, monkey, brain, imaging, immunohistochemistry, glial fibrillary acidic protein (GFAP)

Introduction

Risperidone (Risperdal[®], Janssen Pharmaceutical, Titusville, NJ, USA) is a benzisoxazole-derived second-generation atypical antipsychotic (AAP) drug, approved by the United States Food Drug Administration (U.S. FDA) in 1993, indicated for the treatment of schizophrenia, bipolar disorder, and irritability associated with autistic disorder^{1–3}. The mechanism of action of risperidone is not completely known. It is described as a potent antagonist of serotonin-2

(5-HT₂) and dopamine-2 (D₂) receptors in the brain that demonstrates superior efficacy against the positive (i.e., hallucinations, delusions, racing thoughts) and negative (i.e., apathy, lack of emotions, poor or nonexistent social functioning) symptoms of schizophrenia, with decreased occurrences of extrapyramidal side effects, compared with conventional typical antipsychotics (TAP)^{1, 4, 5}. The U.S. National Institute of Mental Health has identified risperidone as one of the common AAP drugs used in the United States, and it is marketed as Risperdal Consta^{®6, 7}. Risperidone has been ranked in 4th place in efficacy behind the most efficacious drug, clozapine⁸. According to its label, contraindications of risperdal are limited to known hypersensitivity to risperidone, its metabolite paliperidone, or to any excipients in the drug product³. While risperidone has delivered relief to millions of psychiatric patients around the world, it lacks target specificity and is associated with many adverse effects. The warnings and precautions for risperidone are extensive and include cerebrovascular events in elderly patients with dementia-related psychosis, neuroleptic ma-

Received: 12 January 2019, Accepted: 13 May 2019

Published online in J-STAGE: 15 August 2019

*Corresponding authors: G Fernandez

(e-mail: guillermo_fernandez@merck.com)

S Kuruvilla (e-mail: sabu_kuruvilla@merck.com)

©2019 The Japanese Society of Toxicologic Pathology

This is an open-access article distributed under the terms of the Creative Commons Attribution Non-Commercial No Derivatives

(by-nc-nd) License. (CC-BY-NC-ND 4.0: <https://creativecommons.org/licenses/by-nc-nd/4.0/>).



lignand syndrome, tardive dyskinesia, metabolic changes, hyperprolactinemia, orthostatic hypotension, potential for cognitive and motor impairment, and seizures³. Antagonism at receptors other than D₂ and 5HT₂ may explain some of the undesirable effects of risperidone³.

In nonclinical studies, research has been conducted on the long-term behavioral effects of risperidone treatment in rats during early life. One study indicated that the locomotor activity during rat adulthood was permanently modified by early-life risperidone treatment, suggesting that chronic antipsychotic drug use in children for symptoms of autism could modify brain development and alter neural set points for specific behaviors during adulthood⁹. The preclinical toxicology profile of risperidone in rats and dogs has been described in the scientific literature^{10–12}. Risperidone has distinctive behavioral and psychomotor effects in nonhuman primates. Clinical signs of dystonia were observed in Cebus monkeys after dosing intramuscularly at 0.025 to 0.25 mg/kg¹³. Likewise, Cebus monkeys that received 0.01 to 0.25 mg/kg of risperidone intramuscularly developed EPS (e.g., dystonia and Parkinsonism), showed decreased locomotor activity, and seemed calmer than their vehicle counterparts¹⁴. Administration of TAP or AAP drugs in rhesus monkeys induced significant alterations in parameters of social and solitary behaviors¹⁵. In the same study, it was observed that risperidone had nonsedative effects in rhesus monkeys, similar to those observed in the clinical setting¹⁶. Risperidone is known to be brain penetrant, but imaging studies are limited. However, studies using positron emission tomography (PET) estimated that the extent of D₂ receptor occupancy in the monkey brain was approximately 75% after a subcutaneous 0.05 mg/kg dose of risperidone, without discrimination between the striatal (caudate and putamen) and the extrastriatal (thalamus and cortical regions) dopamine receptors¹⁷.

In the context of many adverse effects of risperidone and other antipsychotics, there is a great unmet medical need to develop the next generation of antipsychotics that more specifically target receptors in critical pathways to more effectively treat millions of patients who suffer from specific forms of psychosis, without debilitating or life-threatening adverse effects. The current study was conducted to extend the characterization of the currently published literature to provide a benchmark of the preclinical profile of risperidone in rhesus monkeys. These data provide further context for

a commonly prescribed AAP drug to support the development of new antipsychotics, as there is a paucity of risperidone-related literature in nonhuman primates. The study further sought to characterize risperidone as a prototypical agent to support the understanding of the physiological and neuropathologic effects of these agents. To our knowledge, the brain histomorphology and magnetic resonance imaging (MRI) changes in nonhuman primates treated with risperidone have not previously been reported. We present the results of histomorphology and MRI evaluation of the brain and toxicokinetic analysis of risperidone and its active metabolite, paliperidone, in rhesus monkeys orally exposed to risperidone for 3 weeks, or 3 months followed by a 3-month recovery period. This study provides new data to bridge the gap in the scientific literature, providing insights into the nonclinical risk assessment strategy for new drug candidates with psychiatric indications.

Materials and Methods

The number of animals, procedures, and experimental design were reviewed and approved by our Institutional Animal Care and Use Committee (IACUC). Research was conducted in compliance with the Animal Welfare Act and other federal statutes and regulations relating to animals as stated in the *Guide for Care and Use of Laboratory Animals* (National Research Council 1996). Merck & Co., Inc., Kenilworth, NJ, USA, is fully accredited by the Association for Assessment and Accreditation of Laboratory Animal Care (AAALAC) International.

Study design

Purpose-bred, treatment-naïve, male and female rhesus monkeys (*Macaca mulatta*) (n=22), 2 to 3 years of age, supplied by Mannheimer Foundation, Haman Ranch, LaBelle, Florida, USA, were used in this study. Monkeys were assigned to 6 groups that received risperidone (99.6% pure; Bosche Scientific, New Brunswick, NJ, USA) or vehicle (deionized water) orally by gavage (5 mL/kg) once a day. The study design is summarized in Table 1.

In the risperidone-treated groups (4, 5, and 6), dose escalation was used to acclimate the animals to the pharmacological effects of risperidone and identify the maximum tolerated dose (MTD) in the study (0.5 mg/kg/day). The 1 mg/kg/day dose level was considered a non-tolerated dose based

Table 1. Study Design

Group	#Animals/sex	Dose level	No. of daily doses received	Duration of recovery
1	2F, 2M	0 mg/kg/day (Control) ^a	22 (~3 weeks)	None
2	1F, 1M	0 mg/kg/day (Control) ^a	84 (~3 months)	None
3	2F, 2M	0 mg/kg/day (Control) ^a	84 (~3 months)	~3 months
4	2F, 2M	0.2/1.0/0.2/0.5 mg/kg/day ^b	22 (~3 weeks)	None
5	2F, 2M	0.2/1.0/0.2/0.5 mg/kg/day ^b	84 (~3 months)	None
6	2F, 2M	0.2/1.0/0.2/0.5 mg/kg/day ^b	84 (~3 months)	~3 months

^aVehicle: Deionized water. ^b0.2 mg/kg/day on Days 1–3, 1.0 mg/kg/day on Day 4, 0.2 mg/kg/day on Days 5 and 6, and 0.5 mg/kg/day thereafter. F=female; M=male.

on the severity and duration of the physical signs. Animals were designated for necropsy after approximately 3 weeks or 3 months of dosing. Two groups (3 and 6) dosed for approximately 3 months were terminated following a 3-month recovery (non-dosing) phase. The intent was to maintain the animals at a stable dose (e.g., 0.5 mg/kg/day) for approximately 2 weeks and 3 months, which are common durations of treatment used to assess the nonclinical safety of candidate molecules in drug development programs. Based on the pathological findings from the necropsy, 3 months was estimated to be an appropriate duration of recovery.

During the conduct of the study, the animals were pair housed. The targeted ranges of temperature and humidity were between 21 and 24°C and 30 and 70%, respectively, with a 12-h diurnal light cycle. Temperature and humidity in the rooms were monitored in accordance with the testing facility's standard operating procedures (SOPs). Fresh drinking water was provided *ad libitum*, and monkeys were fed twice daily with LabDiet® Laboratory Fiber-Plus® biscuits (Purina Mills, Inc., Gray Summit, MO, USA) along with produce treats and access to enrichment toys. All animals were observed daily for physical signs.

MRI

Two MRI examinations were conducted to quantify the volumes of the caudate nucleus and putamen. Given that volumetric changes were reported in multiple clinical studies with contradicting results^{18–21}, the sole goal of including an MRI assessment was to assess volumes to better understand the related clinical results. Animals slated for necropsy after 3 months of dosing (groups 2 and 5) and animals slated for recovery (groups 3 and 6) were subjected to MRI at the end of the 3-month dosing period (Exam 1). Each animal in the recovery group (dose groups 3, 6) were again subjected to MRI at the end of the 3-month recovery period (Exam 2). Animals were fasted overnight prior to the MRI sessions.

MRI was performed with a Siemens 3T Trio system using a 32-channel brain coil. To facilitate handling, animals were sedated with ketamine, anesthetized with propofol, and maintained in an anesthetic plane with isoflurane gas. Intravenous Ringer's lactate solution was administered continuously during the procedure to maintain blood volume.

A 3D coronal spoiled gradient echo T1-weighted (T1W) sequence was acquired over the entire brain volume ("MPRAGE" on the Siemens Syngo platform). A T1W sequence was chosen because it is a routine clinical sequence that provides excellent soft tissue contrast between brain structures and grey and white matter. The parameters for the T1W sequence included the following: field of view = 128 × 128 mm, TE = 3.79 ms, TR = 2,300 ms, TI = 870 ms, 256 × 256 matrix, slice thickness = 1.0 mm and distance between slices = 50% for a final resolution of 0.5 × 0.5 × 1.0 mm, 80 or 88 slices depending on the size of the animal, parallel imaging factor = 2, averages = 4, flip angle = 12°, bandwidth = 130 Hz/pixel. The acquisition time for the T1W sequence was 21 min and 20 s.

MRI image analysis

The brain volumes from all animals were analyzed using VivoQuant (v2.5, InviCRO, LLC, Boston, MA, USA). Brain images were segmented to identify the volumes of the left putamen, right putamen, left caudate nucleus, right caudate nucleus, and the remaining whole brain using the software's Whole Body Atlas Tool; this tool uses a template-driven volumetrics approach to segment images based on a user-created atlas of known segmented volumes²². Such a template was created by entering the brain volumes of 6 manually segmented animal brains into the Whole Body Atlas Tool using the group 2 (n=2) and group 3 (n=4) images from Exam 1. The manually segmented brain images and their known volumes were registered to a single exemplary set of images prior to being entered into the atlas. Results from the left and right putamen were combined and reported as the "putamen", and results from the left and right caudate nucleus were combined and reported as the "caudate nucleus".

All 14 brain images from all groups and both time points were then segmented using the user-defined atlas. All segmentations were then peer reviewed by a separate user for correctness, and any edits to the segmentations were performed as needed.

MRI statistical analysis

For volumes acquired during Exam 1, a one-way ANOVA model was applied to the means of each group and the pooled variance to perform between-group analyses. For volumes acquired during Exam 1 and Exam 2 for groups 3 and 6, within-group analyses were performed using a linear mixed-effects model²³. Both the one-way ANOVA and linear mixed-effects modeling were implemented using the R package *autoLDA*. P-values below 0.05 were deemed significant.

Study termination and postmortem examination

Necropsy: Food was withdrawn overnight prior to necropsy. Monkeys were weighed and humanely euthanized by intravenous injection of pentobarbital followed by exsanguination. Necropsy consisted of comprehensive gross evaluation and collection and weighing of the brain. Brain weight data were reviewed as absolute weights and weights as a percent of body weight. Brains were fixed in 10% neutral buffered formalin.

Histopathology examination

Brain (including basal nuclei, cerebral cortex, corpus callosum, internal/external capsule, hypothalamus, amygdala, thalamus, hippocampus, optic tract, midbrain, pons, pyramids, cerebellum, medulla oblongata, and choroid plexus) sections were prepared by routine methods, stained with hematoxylin and eosin (H&E), and examined microscopically. Brain sections taken adjacent to each H&E histology sections were examined microscopically after staining for 1) GFAP (an immunohistochemical stain for intermediate filaments of astrocytes; rabbit polyclonal anti-GFAP antibody,

1:10,000, G9269, MilliporeSigma, Burlington, MA, USA; biotinylated donkey anti-rabbit IgG secondary antibody, 1:500, 711-065-152, Jackson ImmunoResearch Laboratories, West Grove, PA, USA; 3,3'-diaminobenzidine [DAB], K3468, Agilent Dako, Santa Clara, CA, USA; DAB deparaffinization and antigen retrieval, Dewax and HIER buffer L, pH6.0, TA-100-DHBL Thermo Scientific, Waltham, MA, USA), 2) ionized calcium binding adapter molecule 1 (Iba1; an immunohistochemical stain for microglia; rabbit polyclonal anti-Iba1 antibody, 1:500, 019-19741, FUJIFILM Wako Pure Chemical Corporation, Richmond, VA, USA; biotinylated donkey anti-rabbit IgG secondary antibody, 1:1,000, 711-065-152, Jackson ImmunoResearch Laboratories, Dewax and HIER buffer L, pH6.0, TA-100-DHBL, Thermo Scientific), and 3) luxol fast blue (LFB; a histochemical stain for myelin, 0.1% solution, 1328-51-4, Acros Organics) counterstained with cresyl violet (CV; a histochemical stain for Nissl body, 0.1% solution, C5042-10G, MilliporeSigma)²⁴.

Toxicokinetic assessment

Whole blood samples, approximately 0.35 to 0.5 mL/time point/animal, were collected from nonfasted animals (except for samples collected at 7 and 24 h on Day 22, for which they were fasted) from the saphenous vein into EDTA-containing tubes. Samples were collected at 0.5, 1, 2, 4, 7, and 24 h post-dose on Days 1, 4, and 22. All plasma samples from the risperidone-treated animals at each time point and from control animals at 4 h post-dose were analyzed for risperidone and its 9-OH-risperidone metabolite, paliperidone, except for samples collected on Day 22, for which samples from only 2 animals/sex were analyzed.

Bioanalytical methods

Risperidone (MW=410.496 g/mol) and paliperidone (MW=426.495 g/mol) plasma samples were processed using a single-step protein precipitation extraction procedure and liquid chromatography separation followed by triple quadrupole mass spectrometry (LC-MS/MS) detection. Using the LC conditions described by Remmerie *et al.*²⁵, the plasma extracts were injected onto a Thermo BDS Hypersil C8 50 × 3 mm, 3 μm column and chromatographed at room temperature under isocratic elution conditions, separating risperidone and the 9-OH-risperidone metabolite, paliperidone. The column effluents were introduced into a SCIEX API 5000 LC-MS/MS system interfaced with TurboIonSpray using multiple reaction monitoring (MRM) in the positive ion mode. Analyte response was measured by summation of MRM transitions at m/z 411.3 → m/z 191.2, 110.2, and 82.2 for risperidone; m/z 427.2 → m/z 207.0, 109.9, and 81.9 for paliperidone; and m/z 329.2 → m/z 162.1 for the internal standard (IS). MS data acquisition and peak integration was performed using the Sciex Analyst 1.6.2 and MultiQuant 3.0.1 software, respectively. The concentrations of risperidone and paliperidone were determined within Watson LIMS version 7.4.1 using linear 1/x² weighted regression.

Toxicokinetic calculations

Toxicokinetic results were calculated using the Phoenix[®] software, Certara, Princeton, NJ, USA. For individual plasma concentrations that were below the lower limit of quantitation (LLOQ), a value of zero was assigned. Toxicokinetic parameter values (area under the plasma concentration versus time curve [AUC_{0–24 h}], peak concentration [C_{max}], and time of peak concentration [T_{max}]) were estimated from risperidone-treated animals, but only concentration values were reported for control animals. The maximum plasma analyte concentration (C_{max}) was determined from the analyte concentration versus time graph for each animal. Mean C_{max} (± SE) values were calculated from the individual animal values. The time to attain the maximum plasma analyte concentration (T_{max}) was the time at which C_{max} occurred for each animal. Mean T_{max} (± SE) values were calculated from the individual animal values. The AUC_{0–24 h} was calculated as a measure of systemic exposure using the linear trapezoidal rule for each animal. Mean AUC_{0–24 h} (± SE) values were calculated from the individual animal values. On Days 1 and 4, the plasma analyte concentrations at time zero were assigned a value of zero; on Day 22, the plasma analyte concentrations at time zero were assigned a value equal to the minimum observed plasma concentrations during the dose interval for each animal.

Results

Physical signs, food consumption

On Days 1–3 (0.2 mg/kg/day), Day 4 (1 mg/kg), Days 5 and 6 (0.2 mg/kg/day), and Days 7–22 (0.5 mg/kg/day), animals treated with risperidone exhibited physical signs that were generally consistent with the pharmacology of risperidone (antagonism of D₂ and 5HT₂ receptors) and included somnolence, movement disorder (e.g., immobility with rigid posture, decreased activity, trembling) and gastrointestinal signs (e.g., unformed stool). The onset of these physical signs was observed at ~1 h post-dose and for up to ~8 h post-dose, but not the next day before dose administration. The physical signs were transient and reversible. Transient unsatisfactory food consumption (more than 2/3 of food ration remaining) was observed in two females and two males in the risperidone-treated group on Day 5 (0.2/1/0.2 mg/kg/day). Food consumption was satisfactory on all other study days.

MRI examination

An example of an MRI output showing a segmented rhesus monkey brain is shown in Fig. 1 for illustrative purposes.

Based on the MRI examination conducted at the end of the 3-month dosing period (Exam 1), there were no statistically significant differences in brain volume or volumes of the caudate nucleus and putamen between the control and treated groups, as summarized in Table 2 below.

Based on the MRI examination conducted at the end of the 3-month recovery period, there were no statistically sig-

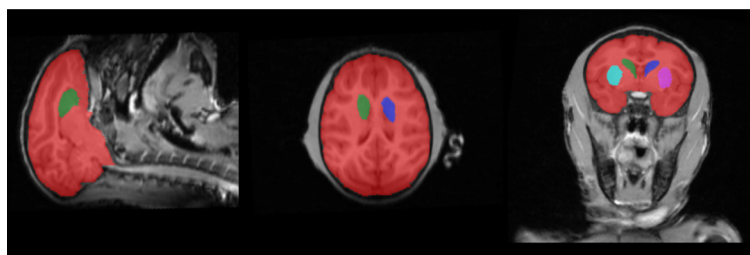


Fig. 1. The image shows the left putamen (cyan), right putamen (pink), left caudate nucleus (green), right caudate nucleus (blue), and remaining whole brain volume (red).

Table 2. Exam 1. Means and Standard Deviations of Brain Volumes and Volumes of the Caudate Nucleus and Putamen (mm^3) for Groups 2, 3, 5, and 6 at the End of the 3-month Dosing

Group	Dose level	Average (mm^3)		
		Whole brain	Caudate nucleus	Putamen
2	0 mg/kg/day (control) (3 mo. dosing)	82,358 \pm 1,463	1,139 \pm 102	1,740 \pm 17
3	0 mg/kg/day (control) (3 mo. dosing/3 mo. recovery)	89,215 \pm 6,629	1,122 \pm 149	1,797 \pm 69
5	0.2/1.0/0.2/0.5 mg/kg/day (3 mo. dosing)	92,557 \pm 6,358	1,250 \pm 75	2,017 \pm 119
6	0.2/1.0/0.2/0.5 mg/kg/day (3 mo. dosing/3 mo. recovery)	86,494 \pm 5,022	1,173 \pm 150	1,964 \pm 169

mo. = months.

Table 3. Exam 2. Means and Standard Deviations of Brain Volumes and Volumes of the Caudate Nucleus and Putamen (mm^3) for Groups 3 and 6 at the End of the 3-month Recovery Period

Group	Dose level	Average \pm sd (mm^3)		
		Whole brain	Caudate nucleus	Putamen
3	0 mg/kg/day (3 mo. dosing/3 mo. recovery)	89,940 \pm 6,642	1,130 \pm 160	1,787 \pm 90
6	0.2/1.0/0.2/0.5 mg/kg/day (3 mo. dosing/3 mo. recovery)	86,799 \pm 5,865	1,130 \pm 202	1,787 \pm 205

mo. = months.

nificant differences in brain volume or volumes of the caudate nucleus and putamen between the control and treated groups, as summarized in Table 3.

Postmortem evaluation

All monkeys survived to scheduled terminations. There were no risperidone-related gross findings or brain weight changes (data not included). Histomorphological evaluation of H&E-, Iba1-, and LFB/CV-stained sections of brain showed no difference between control and risperidone-treated animals. No neuronal necrosis, notable difference in the numbers of neurons or glial cells, aggregations of glial cells, vacuolation in the neuropil, or changes in myelination were observed (Fig. 2). Histomorphologic evaluation of GFAP-stained sections of brain showed a moderate qualitative increase in the GFAP staining of astrocyte cell bodies and processes within the putamen (a region of the dorsal striatum of basal nuclei), without apparent alterations in num-

bers or distribution of astrocytes, in the risperidone-treated group after dosing for 3 weeks or 3 months. The increase in the duration of dosing from 3 weeks to 3 months did not have a noticeable effect on the severity of the change. Based on qualitative assessment, the increased GFAP staining was not apparent in sections of the other brain regions examined. Increased GFAP staining was not observed in monkeys after a 3-month recovery period following 3 months of dosing (Fig. 3). The results are summarized in Table 4.

Toxicokinetics

The mean plasma toxicokinetic parameters for risperidone and its 9-OH-risperidone metabolite, paliperidone, are presented in Table 5.

Plasma toxicokinetic profile

For risperidone, the mean C_{max} values for both sexes at all dose levels were achieved between 0.5 and 0.63 h post-

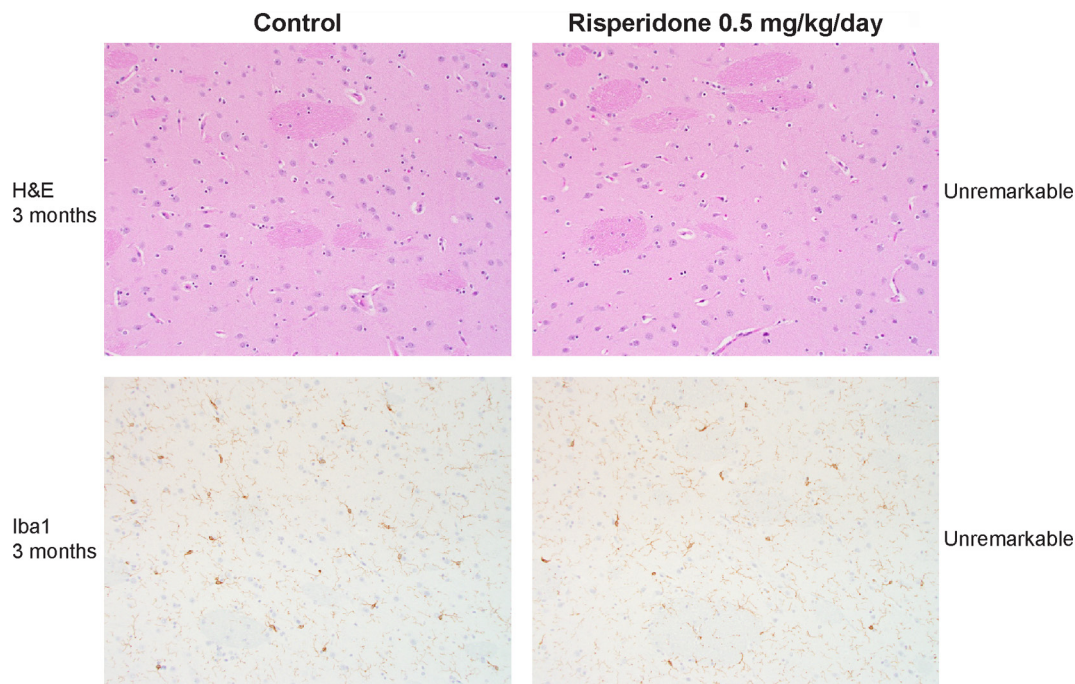


Fig. 2. Brain, putamen: control and risperidone-treated monkeys stained with hematoxylin and eosin (H&E) and ionized calcium binding adapter molecule (Iba1) at the end of the 3-month treatment period. The brain was unremarkable, with no findings, including neuronal necrosis or gliosis, was observed.

dose, followed by rapid plasma elimination, with mean 24-h levels below 3% of their respective mean C_{\max} . For paliperidone, the mean C_{\max} values for both sexes at all doses were achieved between 0.75 and 1.3 h post-dose, followed by rapid plasma elimination, with mean 24-h levels below 3% of their respective mean C_{\max} .

Sex differences in exposure

At 0.2 mg/kg/day, plasma risperidone concentrations in females were below the lower limit of quantitation (LLQ=0.005 μM) at the first two time points (0.5 and 1 h); therefore, no systemic exposure ($\text{AUC}_{0-24\text{ h}}$) could be determined for the females at 0.2 mg/kg/day. At 0.5 mg/kg/day, mean $\text{AUC}_{0-24\text{ h}}$ was approximately 2.4-fold greater in females than in males, while mean C_{\max} was not substantially (more than 2-fold) different between the sexes. However, at 1 mg/kg/day, the mean systemic exposure and C_{\max} were approximately 2.6- and 4.4-fold greater, respectively, in males than in females. For the 9-OH-risperidone metabolite, paliperidone, the mean systemic exposure and C_{\max} were approximately 2.2-fold greater in males than in females at 0.2 mg/kg/day and 1 mg/kg/day, whereas at 0.5 mg/kg/day, these parameters were similar in both sexes.

Dose effects on toxicokinetics

Due to the generally low plasma levels at all doses and to the high inter-animal variability, the mean systemic exposure and C_{\max} values for risperidone did not have dose relationships. It was concluded that mean systemic exposure

and C_{\max} values for paliperidone were approximately dose proportional between 0.2 mg/kg/day and 1 mg/kg/day in both sexes.

Parent to metabolite ratio

Risperidone metabolite to Risperidone $\text{AUC}_{0-24\text{ h}}$ ratios increased with dose from approximately 6 to 17 in both sexes.

Discussion

The neurological clinical signs observed in monkeys in this study were as expected, based on the pharmacology of risperidone, and similar to those reported in human subjects as described in the literature^{4, 13-15}. The two MRI examinations conducted in this study to quantify the volumes of the caudate nucleus and putamen, the regions of the brain previously reported to be altered or suspected to be altered by AAP treatment in humans, did not show meaningful risperidone-associated changes. Reports of investigations on the volumetric effects of antipsychotics on the dorsal striatum in schizophrenia patients have been mixed. While some investigators have reported an increase in the volumes of the caudate nucleus and putamen, associated with risperidone treatment in schizophrenia patients, others have not observed such correlation¹⁸⁻²¹, consistent with our findings in monkeys. In a systematic review of previously published studies, Ebdrup *et al.*¹⁹ indicated that the first- or second-generation antipsychotics caused changes in the

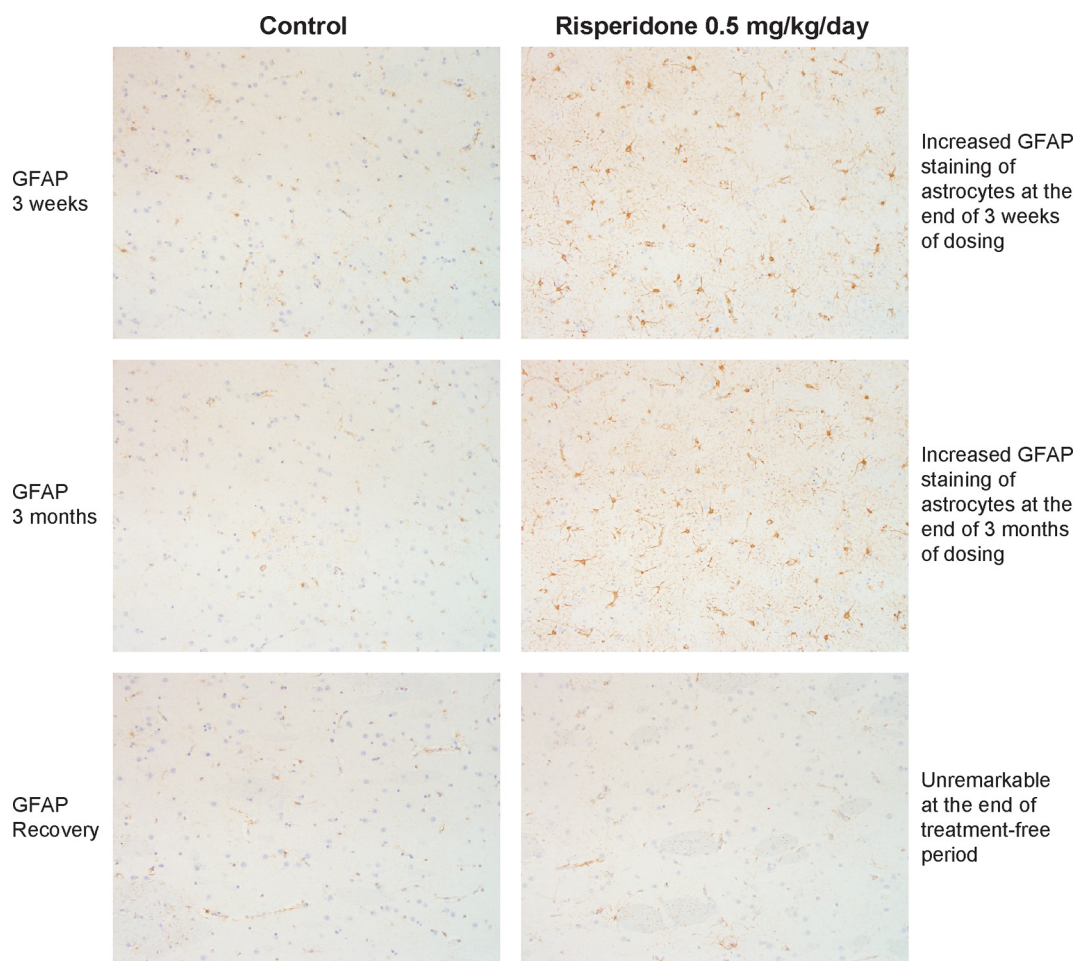


Fig. 3. Brain, putamen: control and risperidone-treated monkeys stained with glial fibrillary acidic protein (GFAP) at the end of the 3-week and 3-month treatment periods and at the end of a 3-month treatment-free period following 3 months of treatment. Increased GFAP staining of the astrocyte cell body and processes was observed in the putamen of the monkeys treated with risperidone after treatment for 3 weeks and 3 months. The increased GFAP staining was not observed at the end of the treatment-free period.

Table 4. Risperidone-related Histomorphologic Findings (Sexes Combined)

Group	1	4	2	5	3	6
Dosing period	~3 weeks		~3 months		~3 months	
Recovery period	-		-		~3 months	
Dose, mg/kg/day	0	0.5	0	0.5	0	0.5
Number of animals	4	4	2	4	4	4
Histomorphology (Incidence)						
Brain						
Astrocyte, increased GFAP staining	0	4	0	3	0	0

volume of the basal ganglia, but some of the reported findings contradicted one another. Many other prospective studies have found positive associations between antipsychotic treatment and the volumes of basal ganglia or gray matter. Emsley *et al.*²¹ found that acute treatment with risperidone or flupenthixol caused a bilateral increase in the volume of the caudate nucleus, compared with that in control patients. Similarly, Hutcheson *et al.*²⁰ reported a positive association of the volume of the caudate nucleus with treatment that

contributed to the variance in treatment response, after controlling for other factors. Finally, Lee *et al.*²⁶ found a positive correlation between risperidone treatment and volumes of several brain regions (left and right putamen, left par hippocampal gyrus, and left amygdala) in Alzheimer’s Disease patients. While MRI is a commonly used clinical tool for monitoring changes in brain anatomy and function, data from our study indicates that the alterations in the microanatomy of the brain associated with risperidone treat-

Table 5. Summary of the Mean (\pm SE) Plasma Risperidone and Paliperidone Toxicokinetic Parameters in Monkeys Following Administration of Risperidone

Day	Dose of risperidone (mg/kg/day)	Analyte	Sex	AUC _{0-24h} (μ M*h)	C _{max} (μ M)	T _{max} (h)
1	0.2	Risperidone	Female	NC	NC	NC
			Male	0.41 \pm ID	0.40 \pm ID	0.50 \pm ID
		Paliperidone	Female	1.10 \pm 0.23	0.28 \pm 0.06	0.75 \pm 0.14
			Male	2.56 \pm 1.31	0.63 \pm 0.27	0.75 \pm 0.14
4	1	Risperidone	Female	0.33 \pm 0.10	0.15 \pm 0.03	0.63 \pm 0.13
			Male	0.87 \pm 0.34	0.65 \pm 0.20	0.50 \pm 0.0
		Paliperidone	Female	5.57 \pm 0.86	1.02 \pm 0.09	1.3 \pm 0.25
			Male	12.5 \pm 3.88	2.31 \pm 0.46	0.75 \pm 0.14
22	0.5	Risperidone	Female	0.40 \pm ID	0.23 \pm ID	0.50 \pm ID
			Male	0.17 \pm ID	0.16 \pm ID	0.50 \pm ID
		Paliperidone	Female	4.61 \pm ID	0.96 \pm ID	0.75 \pm ID
			Male	3.95 \pm ID	0.92 \pm ID	1.0 \pm ID

NC = not calculated due to less than 3 consecutive timepoints above LLQ. ID = insufficient data.

ment in healthy monkeys, as determined by histomorphology evaluation, may be too minimal to be captured by MRI analysis. Therefore, the value of routine structural MRI as an appropriate tool to monitor the striatum of the brains of preclinical species, in the context of the development of antipsychotic drugs, may be limited.

In humans, rats, and dogs, risperidone is metabolized to the active metabolite 9-hydroxy-risperidone (also known as paliperidone) through alicyclic hydroxylation at the 9-position of the tetrahydro-4H-pyrido[1,2-a]-pyrimidin-4-one moiety as the main metabolic pathway. Paliperidone is the main metabolite in plasma^{27, 28}. Data on the pharmacokinetic profile of risperidone in rhesus monkeys are limited. The current work has confirmed the presence of the active metabolite of risperidone, paliperidone (9-hydroxy-risperidone), in rhesus monkey plasma, thereby validating the non-human primate as a suitable model for exploring the imaging and histomorphology profiles of this AAP agent. The pharmacokinetic data generated in this study for risperidone and paliperidone in rhesus monkeys corroborates previous observations in the literature²⁹. The monkey plasma risperidone/paliperidone exposures at 0.2, 1, and 0.5 mg/kg/day were approximately 5.6-29/5.2-60-, 0.6-3.1/5.0-57-, and 0.5-2.4/undetermined-fold higher than the plasma exposures in humans at a therapeutic dose of 1 mg in extensive, intermediate, and poor metabolizers, respectively.

The observation of increased GFAP staining in the cell bodies and processes of astrocytes in the putamen in monkeys treated with risperidone for 3 weeks or 3 months was not accompanied by apparent alterations in the numbers or distribution of astrocytes. Additionally, the distribution of astrocytes showing increased GFAP staining was not consistent with an astroglial response to neuronal loss, in which aggregation or "clustering" of astrocytes and other glial cells occurs in the affected regions³⁰. Scientific literature on the histomorphological changes in the brain of animals exposed to antipsychotic drugs is limited. In rhesus monkeys treated with 0.2 mg/kg of risperidone orally for 6 months, a decrease in the neuronal density of brain cortical layers

II and V was observed by stereology³¹. In the same study, risperidone increased the glial density in cortical layers that receive dense excitatory afferent fibers (layers I and IV) by as much as 33%. Treatment of albino rats with a TAP (chlorpromazine or haloperidol) or AAP (risperidone, olanzapine, or ziprasidone) drug for 30 days increased GFAP reactivity in all examined regions based on IHC staining for GFAP³². Likewise, significantly increased GFAP staining was observed in the cortex (dorsolateral [area 90]) of brains from patients with histories of long-term antipsychotic drug treatment³³.

The increased GFAP staining of astrocytes observed in our study was similar in character to those observed following administration of several typical and atypical antipsychotic drugs, including risperidone, to rats or humans. Blázquez et al. observed increased GFAP reactivity of several areas of the brain (striatum, accumbens, hippocampus, amygdala, cingulate cortex, or hypothalamus) after treating rats with TAP (chlorpromazine and haloperidol) and AAP (risperidone, olanzapine, and ziprasidone) drugs for 30 days³². Toro *et al.* used immunoautoradiography to measure glutamine synthetase (GS), the glial enzyme which recycles synaptic glutamate, as a more direct test of glial mechanisms of abnormal glutamate function in schizophrenia and compared GS with GFAP immunoautoradiography in the dorsolateral (area 9) and orbitofrontal (area 11/47) cortex of the human brain. An increase in GFAP immunoreactivity was observed in area 9 that significantly correlated with lifetime antipsychotic drug treatment³³. To our knowledge, this is the first report demonstrating increased GFAP staining in the brain of monkeys administered an AAP drug.

The various functions of astrocytes in the brain include the metabolism of neurotransmitters such as glutamate³⁴⁻⁴². Studies have indicated that schizophrenia and other related neuropsychiatric conditions are associated with elevation of glutamate metabolites in various brain regions due to dysregulation of glutamate transporters, and treatment with antipsychotics, including risperidone, has resulted in significant reduction of glutamate metabolites in various brain

regions, including the striatum, of patients^{43–45}. Further, risperidone was shown to induce significantly higher uptake of glutamate and increased glutathione synthase activity in the C6 astroglial cell line⁴⁶. Taking into consideration the increased burden of glutamate metabolism placed on astrocytes due to risperidone treatment; the absence of neuronal loss as indicated by the results of the H&E and CV staining, lack of demyelination as indicated by the results of the LFB staining, and the absence of neural scarring/microgliosis as shown by the Iba1 staining; and the context of the expected prolonged presence of reactive astrocytes and microglia in the brain following neuronal injury^{47, 48}, the increase in GFAP expression observed in the current study was considered an adaptive, non-adverse change associated with the pharmacology of risperidone. The complete reversibility of both the GFAP expression profile and neurological physical signs support the adaptive nature of the brain change in these monkeys treated with risperidone. The absence of treatment-associated brain pathology further supports the non-adverse nature of the brain change. The findings in this study help further increase our understanding of the effects of subacute to chronic treatment with AAP drugs on the nonhuman primate brain. While risperidone increased the GFAP staining of astrocytes in the striatum, this adaptive response did not lead to permanent morphologic alterations in the brain, as evidenced by the absence of increased GFAP staining in monkeys after a 3-month recovery period. This observation is a valuable consideration in the nonclinical de-risking of drug candidates during the development of new treatments for psychiatric disorders.

Funding: This work was supported by Merck Sharp & Dohme Corp., a subsidiary of Merck & Co., Inc., Kenilworth, NJ, USA.

Role of the Funding Source: This work was funded by Merck Sharp & Dohme Corp., a subsidiary of Merck & Co., Inc., Kenilworth, NJ, USA. Authors and others employed by the sponsor contributed to study design, collection, analysis, and interpretation of data; writing of the report; and in the decision to submit the article for publication. All authors contributed to study conception, design, and planning; GF, CH, SK, JM, and FP acquired and analyzed data; and GF, CH, SK, FP, and TF interpreted the results. GF, CH, SK, JM, FP, TF, and RB contributed to drafting and reviewing the manuscript; all authors critically revised the manuscript for important intellectual content and approved the final version of the manuscript.

Disclosure of Potential Conflicts of Interest: This work was supported by Merck Sharp & Dohme Corp., a subsidiary of Merck & Co., Inc., Kenilworth, NJ, USA. GF, CH, SK, JM, FP, TF, and RB are employees of Merck Sharp & Dohme Corp., a subsidiary of Merck & Co., Inc., Kenilworth, NJ, USA, and own stock or hold stock options in Merck & Co., Inc., Kenilworth, NJ, USA. Authors employed by Merck Sharp & Dohme Corp., a subsidiary of Merck &

Co., Inc., Kenilworth, NJ, USA, participated in the study design, collection, analysis, and interpretation of data, writing of the report, and in the decision to submit the article for publication.

Acknowledgments: The authors thank the following MSD colleagues for their valuable contributions to this research project: Amy McCue, Joseph Knox, Claudette Lazarus, Tracy Strowger, and Dawn Toros in the Toxicological Sciences laboratory for their support of the dosing, formulation preparation, data collection, and imaging procedures; Brian McCullough for coordination of all pathology activities; Caron Leach, Phil Manfre, Tara McNutt, and Christine Reichard for their efforts in the immunohistochemical/histochemical staining of brains; and Jason Flor for capturing the photomicrographs.

References

- Colpaert FC. Discovering risperidone: the LSD model of psychopathology. *Nat Rev Drug Discov.* **2**: 315–320. 2003. [Medline] [CrossRef]
- Möller HJ. Risperidone: a review. *Expert Opin Pharmacother.* **6**: 803–818. 2005. [Medline] [CrossRef]
- Label for Risperdal. 2009, from United States Food and Drug Administration (US FDA) website: https://www.accessdata.fda.gov/drugsatfda_docs/label/2009/020272s056,020588s044,021346s033,021444s031bl.pdf.
- Uthayathas S, Shaffer CL, Menniti FS, Schmidt CJ, and Papa SM. Assessment of adverse effects of neurotropic drugs in monkeys with the “drug effects on the nervous system” (DENS) scale. *J Neurosci Methods.* **215**: 97–102. 2013. [Medline] [CrossRef]
- Love RC, and Nelson MW. Pharmacology and clinical experience with risperidone. *Expert Opin Pharmacother.* **1**: 1441–1453. 2000. [Medline] [CrossRef]
- National Institute of Mental Health Antipsychotics. Website: https://www.nimh.nih.gov/health/topics/mental-health-medications/index.shtml#part_149866.
- Johnson & Johnson Investor Relations SEC Filings Website <http://www.investor.jnj.com/sec.cfm>.
- Leucht S, Cipriani A, Spineli L, Mavridis D, Orey D, Richter F, Samara M, Barbui C, Engel RR, Geddes JR, Kissling W, Stapf MP, Lässig B, Salanti G, and Davis JM. Comparative efficacy and tolerability of 15 antipsychotic drugs in schizophrenia: a multiple-treatments meta-analysis. *Lancet.* **382**: 951–962. 2013. [Medline] [CrossRef]
- Bardgett ME, Franks-Henry JM, Colemire KR, Juneau KR, Stevens RM, Marczinski CA, and Griffith MS. Adult rats treated with risperidone during development are hyperactive. *Exp Clin Psychopharmacol.* **21**: 259–267. 2013. [Medline] [CrossRef]
- Baptista T, Araujo de Baptista E, Ying Kin NM, Beaulieu S, Walker D, Joobar R, Lalonde J, and Richard D. Comparative effects of the antipsychotics sulpiride or risperidone in rats. I: bodyweight, food intake, body composition, hormones and glucose tolerance. *Brain Res.* **957**: 144–151. 2002. [Medline] [CrossRef]
- Ota M, Mori K, Nakashima A, Kaneko YS, Fujiwara K, Itoh M, Nagasaka A, and Ota A. Peripheral injection of ris-

- peridone, an atypical antipsychotic, alters the bodyweight gain of rats. *Clin Exp Pharmacol Physiol*. **29**: 980–989. 2002. [[Medline](#)] [[CrossRef](#)]
12. Tian J, Wang W, Ye L, Cen X, Guan X, Zhang J, Yu P, Du G, Liu W, and Li Y. A 12-week intramuscular toxicity study of risperidone-loaded microspheres in Beagle dogs. *Hum Exp Toxicol*. **33**: 473–487. 2014. [[Medline](#)] [[CrossRef](#)]
 13. Casey DE. Serotonergic and dopaminergic aspects of neuroleptic-induced extrapyramidal syndromes in nonhuman primates. *Psychopharmacology (Berl)*. **112**(Suppl): S55–S59. 1993. [[Medline](#)] [[CrossRef](#)]
 14. Casey DE. Behavioral effects of sertindole, risperidone, clozapine and haloperidol in Cebus monkeys. *Psychopharmacology (Berl)*. **124**: 134–140. 1996. [[Medline](#)] [[CrossRef](#)]
 15. Kumar R, Palit G, and Dhawan BN. Comparative behavioural effects of typical and atypical antipsychotic drugs in rhesus monkey. *Eur J Pharmacol*. **462**: 133–138. 2003. [[Medline](#)] [[CrossRef](#)]
 16. Marder SR, and Meibach RC. Risperidone in the treatment of schizophrenia. *Am J Psychiatry*. **151**: 825–835. 1994. [[Medline](#)] [[CrossRef](#)]
 17. Mukherjee J, Christian BT, Narayanan TK, Shi B, and Mantil J. Evaluation of dopamine D-2 receptor occupancy by clozapine, risperidone, and haloperidol in vivo in the rodent and nonhuman primate brain using 18F-fallypride. *Neuropsychopharmacology*. **25**: 476–488. 2001. [[Medline](#)] [[CrossRef](#)]
 18. Mamah D, Wang L, Barch D, de Erausquin GA, Gado M, and Csernansky JG. Structural analysis of the basal ganglia in schizophrenia. *Schizophr Res*. **89**: 59–71. 2007. [[Medline](#)] [[CrossRef](#)]
 19. Ebdrup BH, Nørbak H, Borgwardt S, and Glenthøj B. Volumetric changes in the basal ganglia after antipsychotic monotherapy: a systematic review. *Curr Med Chem*. **20**: 438–447. 2013. [[Medline](#)]
 20. Hutcheson NL, Clark DG, Bolding MS, White DM, and Lahti AC. Basal ganglia volume in unmedicated patients with schizophrenia is associated with treatment response to antipsychotic medication. *Psychiatry Res*. **221**: 6–12. 2014. [[Medline](#)] [[CrossRef](#)]
 21. Emsley R, Asmal L, du Plessis S, Chiliza B, Kidd M, Carr J, and Vink M. Dorsal striatal volumes in never-treated patients with first-episode schizophrenia before and during acute treatment. *Schizophr Res*. **169**: 89–94. 2015. [[Medline](#)] [[CrossRef](#)]
 22. Warfield SK, Robatino A, Dengler J, Jolesz FA, and Kikinis R. Nonlinear registration and template driven segmentation. *Brain Warping*. **4**: 67–84. 1988.
 23. Pinheiro JC, and Bates DM. *Mixed-effects Models in S and S-PLUS*. Springer, New York. 2004.
 24. Bolon B, Garman RH, Pardo ID, Jensen K, Sills RC, Roulois A, Radovsky A, Bradley A, Andrews-Jones L, Butt M, and Gumprecht L. STP position paper: Recommended practices for sampling and processing the nervous system (brain, spinal cord, nerve, and eye) during nonclinical general toxicity studies. *Toxicol Pathol*. **41**: 1028–1048. 2013. [[Medline](#)] [[CrossRef](#)]
 25. Remmerie BM, Sips LL, de Vries R, de Jong J, Schothuis AM, Hooijschuur EW, and van de Merbel NC. Validated method for the determination of risperidone and 9-hydroxyrisperidone in human plasma by liquid chromatography-tandem mass spectrometry. *J Chromatogr B Analyt Technol Biomed Life Sci*. **783**: 461–472. 2003. [[Medline](#)] [[CrossRef](#)]
 26. Lee YM, Park JM, Lee BD, Moon E, Jeong HJ, Chung YI, Kim JH, Kim HJ, Mun CW, Kim TH, and Kim YH. Gray matter volumes and treatment response of psychotic symptoms to risperidone in antipsychotic-naïve Alzheimer's disease patients. *J Clin Psychiatry*. **77**: e8–e13. 2016. [[Medline](#)] [[CrossRef](#)]
 27. Mannens G, Huang ML, Meuldermans W, Hendrickx J, Woestenborghs R, and Heykants J. Absorption, metabolism, and excretion of risperidone in humans. *Drug Metab Dispos*. **21**: 1134–1141. 1993. [[Medline](#)]
 28. Meuldermans W, Hendrickx J, Mannens G, Lavrijsen K, Janssen C, Bracke J, Le Jeune L, Lauwers W, and Heykants J. The metabolism and excretion of risperidone after oral administration in rats and dogs. *Drug Metab Dispos*. **22**: 129–138. 1994. [[Medline](#)]
 29. Muly EC, Votaw JR, Ritchie J, and Howell LL. Relationship between dose, drug levels, and D2 receptor occupancy for the atypical antipsychotics risperidone and paliperidone. *J Pharmacol Exp Ther*. **341**: 81–89. 2012. [[Medline](#)] [[CrossRef](#)]
 30. Maxie MG, and Youssef S. Nervous system. In: Jubb, Kennedy and Palmer's pathology of domestic animals, 5th ed. MG Maxie (ed), Elsevier Health Sciences, London. 289–297. 2007.
 31. Selemon LD, Lidow MS, and Goldman-Rakic PS. Increased volume and glial density in primate prefrontal cortex associated with chronic antipsychotic drug exposure. *Biol Psychiatry*. **46**: 161–172. 1999. [[Medline](#)] [[CrossRef](#)]
 32. Blázquez Arroyo JL, Fraile Malmierca E, Casadiego Cubides A, Llorca Ramón G, and Ledesma Jimeno A. Glial reactivity after antipsychotic treatment. An experimental study in rats and its implications for psychiatry. *Actas Esp Psiquiatr*. **38**: 278–284. 2010. [[Medline](#)]
 33. Toro CT, Hallak JEC, Dunham JS, and Deakin JFW. Glial fibrillary acidic protein and glutamine synthetase in subregions of prefrontal cortex in schizophrenia and mood disorder. *Neurosci Lett*. **404**: 276–281. 2006. [[Medline](#)] [[CrossRef](#)]
 34. Kimelberg HK, and Nedergaard M. Functions of astrocytes and their potential as therapeutic targets. *Neurotherapeutics*. **7**: 338–353. 2010. [[Medline](#)] [[CrossRef](#)]
 35. Takahashi N, and Sakurai T. Roles of glial cells in schizophrenia: possible targets for therapeutic approaches. *Neurobiol Dis*. **53**: 49–60. 2013. [[Medline](#)] [[CrossRef](#)]
 36. Hertz L. Intercellular metabolic compartmentation in the brain: past, present and future. *Neurochem Int*. **45**: 285–296. 2004. [[Medline](#)] [[CrossRef](#)]
 37. Bak LK, Schousboe A, and Waagepetersen HS. The glutamate/GABA-glutamine cycle: aspects of transport, neurotransmitter homeostasis and ammonia transfer. *J Neurochem*. **98**: 641–653. 2006. [[Medline](#)] [[CrossRef](#)]
 38. Schousboe A, Sarup A, Bak LK, Waagepetersen HS, and Larsson OM. Role of astrocytic transport processes in glutamatergic and GABAergic neurotransmission. *Neurochem Int*. **45**: 521–527. 2004. [[Medline](#)] [[CrossRef](#)]
 39. Chaudhry FA, Lehre KP, van Lookeren Campagne M, Ottersen OP, Danbolt NC, and Storm-Mathisen J. Glutamate transporters in glial plasma membranes: highly differentiated localizations revealed by quantitative ultrastructural

- immunocytochemistry. *Neuron*. **15**: 711–720. 1995. [[Medline](#)] [[CrossRef](#)]
40. Rothstein JD, Martin L, Levey AI, Dykes-Hoberg M, Jin L, Wu D, Nash N, and Kuncel RW. Localization of neuronal and glial glutamate transporters. *Neuron*. **13**: 713–725. 1994. [[Medline](#)] [[CrossRef](#)]
41. Norenberg MD, and Martinez-Hernandez A. Fine structural localization of glutamine synthetase in astrocytes of rat brain. *Brain Res*. **161**: 303–310. 1979. [[Medline](#)] [[CrossRef](#)]
42. Bröer S, and Brookes N. Transfer of glutamine between astrocytes and neurons. *J Neurochem*. **77**: 705–719. 2001. [[Medline](#)] [[CrossRef](#)]
43. Egerton A, Bhachu A, Merritt K, McQueen G, Szulc A, and McGuire P. Effects of antipsychotic administration on brain glutamate in schizophrenia: A systematic review of longitudinal ¹H-MRS studies. *Front Psychiatry*. **8**: 66. 2017. [[Medline](#)] [[CrossRef](#)]
44. O'Donovan SM, Sullivan CR, and McCullumsmith RE. The role of glutamate transporters in the pathophysiology of neuropsychiatric disorders. *NPJ Schizophr*. **3**: 32. 2017. [[Medline](#)] [[CrossRef](#)]
45. de la Fuente-Sandoval C, León-Ortiz P, Azcárraga M, Stephano S, Favila R, Díaz-Galvis L, Alvarado-Alanis P, Ramírez-Bermúdez J, and Graff-Guerrero A. Glutamate levels in the associative striatum before and after 4 weeks of antipsychotic treatment in first-episode psychosis: a longitudinal proton magnetic resonance spectroscopy study. *JAMA Psychiatry*. **70**: 1057–1066. 2013. [[Medline](#)] [[CrossRef](#)]
46. Quincozes-Santos A, Bobermin LD, Kleinkauf-Rocha J, Souza DO, Riesgo R, Gonçalves CA, and Gottfried C. Atypical neuroleptic risperidone modulates glial functions in C6 astroglial cells. *Prog Neuropsychopharmacol Biol Psychiatry*. **33**: 11–15. 2009. [[Medline](#)] [[CrossRef](#)]
47. McGeer PL, Schwab C, Parent A, and Doudet D. Presence of reactive microglia in monkey substantia nigra years after 1-methyl-4-phenyl-1,2,3,6-tetrahydropyridine administration. *Ann Neurol*. **54**: 599–604. 2003. [[Medline](#)] [[CrossRef](#)]
48. Barcia C, Sánchez Bahillo A, Fernández-Villalba E, Bautista V, Poza Y Poza M, Fernández-Barreiro A, Hirsch EC, and Herrero MT. Evidence of active microglia in substantia nigra pars compacta of parkinsonian monkeys 1 year after MPTP exposure. *Glia*. **46**: 402–409. 2004. [[Medline](#)] [[CrossRef](#)]